Effect of Friction Welding Parameters on Mechanical and Microstructural Properties of Dissimilar AISI 1010-ASTM B22 Joints

In this study, the characteristic of structures, tensile properties, hardness values, and microstructural changes of friction joints were investigated

BY A. KURT, I. UYGUR, AND U. PAYLASAN

ABSTRACT

Rotary friction welding is one of the most economical and efficient production methods for joining similar and dissimilar materials. It is widely used with metals and thermoplastics in a wide variety of aviation, transport, and aerospace industrial component designs. Individually, mild steel to mild steel and copper to copper are normally easy to weld by fusion welding methods, but the joint of mild steel to copper can be extremely difficult due to the differences in the two materials' melting temperature, density, strength, and thermal conductivity. Thus, these kinds of problems can be eliminated by a solid-state friction welding technique. Hence, the current study attempts to understand the friction welding characteristics of mild steel-bronze dissimilar parts. This study looks into the influence of process parameters, which includes friction pressure, upsetting pressure, and upset time on the axial shortening, hardness, microstructure, and tensile properties of the welds. The optimum parameters for upset time, upset pressure, and friction pressure necessary for welding were obtained. Finally, the obtained mechanical properties results were commented on the light of optical microscopy.

Introduction

Welding of machinery components is compulsory in most engineering applications. Just a few decades ago, materials were classified as weldable and nonweldable, but innovations in technology allowed joining of most materials by fusion and solid-state welding techniques. Typical fusion welding techniques include gas welding (oxyacetylene), arc welding (shielded metal, gas tungsten, and submerged), and high-energy beam welding (electron and laser). Heat sources for these techniques are a gas flame, an electric arc, and a high beam, respectively. However, in the nature of these techniques, excessive heating can cause damage to the workpiece, including weakening and distortion. Some of the fusion techniques are applied for various materials (Refs. 1–3). Low carbon (mild) steel and copper alloys are widely applied prospects because of their economic value, plus good mechanical and physical properties. It is an easy process to weld these materials by themselves. Unfortunately, most engineering materials have to join with dissimilar counterparts. Thus, it is difficult to obtain good-quality weld joints using molten welding methods. Some defects and intermetallic phases can occur during the process because of the great differences between Fe and Cu in physical, mechanical, and chemical properties. Table 1 shows some physical and mechanical properties of AISI 1010 mild steel and ASTM B22 copper bronze (Ref. 4). These metals have good electrical and heat conductivity and have a good ability for casting and machining. In order to take advantage of the dissimilar metals involved, it is necessary to produce high-quality joints between them. Typical solid-state joining applications of diffusion welding for various content of the aluminum metal matrix composites (Refs. 5–7) and friction stir welding (Ref. 8) have been studied in detail. Welding copper alloys is usually difficult using a conventional fusion welding process because copper has high thermal diffusivity, which is about 10 to 100 times higher than in many steels and nickel alloys. The effects of diffusion welding parameters on the mechanical response of low carbon steel and commercially pure copper were studied in detail by Kurt et al. (Ref. 5). Welding time, applied load, welding temperature, and chemical composition of the steel are some of the key parameters to controlling the solid-state diffusion welding process.

Rotary friction welding is one of the solid-state techniques that is applied to the joining of similar and dissimilar counterparts. In this technique, machinery components are brought into contact. While one of them remains stationary, the other is rotated with the applied pressure. When the temperature of the interfaces has reached an optimum value for the extensive plastic deformation, the rotation is stopped, while the forging pressure remains unchanged or increased. The application of an axial force maintains intimate contact between the parts and causes plastic deformation of the material near the weld interface. If sufficient frictional heat has been produced during softening, larger wear particles begin to expel from the interfaces and axial shortening of the components begin as a result of the expelled upsetting. In general, heat is conducted away from the interfaces, and a plastic zone develops. The plasticized layer is formed on the interfaces and the local stress system with the assistance of the rotary movement extrudes material from the interface into the flash. It has been shown that weld integrity is strongly affected by the rate of flash expelled under

KEYWORDS

Friction Welding
Mild Steel-Bronze
Welding Parameters
Mechanical Properties

A. KURT is with Gazi University, Faculty of Technology, Ankara-Turkey. I. UYGUR (ilyasuygur@duzce.edu.tr) *is with Duzce University, Faculty of Engineering, Duzce, Turkey. U. PAYLASAN is with Korfez Vocational and Technical High School, Kocaeli, Turkey.*

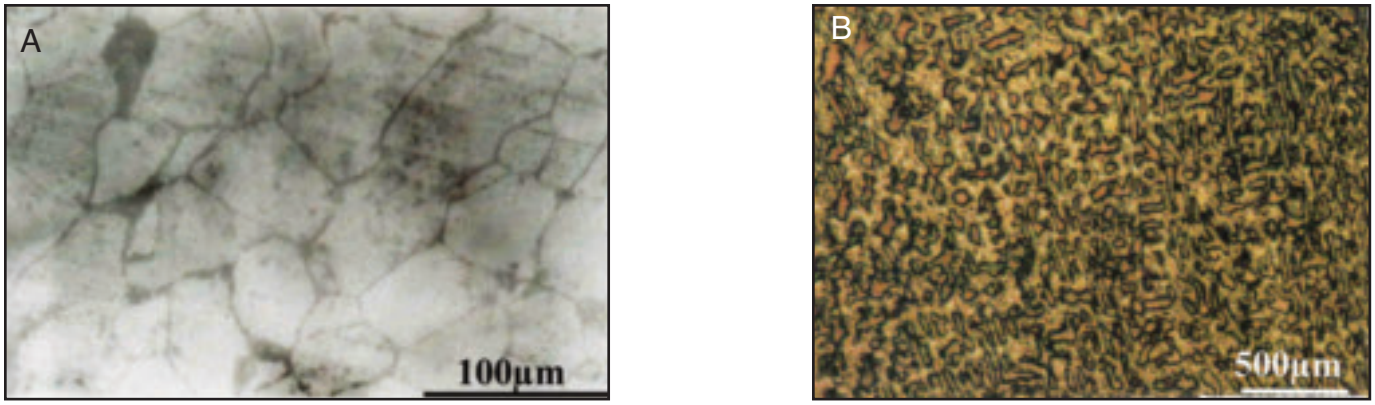

Fig. 1 — Microstructure of A — AISI 1010 steel (× 500); B — ASTM B22 copper bronze (× 50).

appropriate conditions (Ref. 9). Friction welding has a lot of advantages over other welding processes, such as no melting, high reproducibility, short production time, low energy input, limited heat-affected zone (HAZ), avoidance of porosity formation and grain growth, and the use of nonshielding gases during the welding process. Also, the technique is not only applied to round specimens but used for rectangular components. It is called linear friction welding and has recently been applied to steel (Ref. 10).

Although a large amount of previous studies (Refs. 7–11) in similar and dissimilar materials have been studied, mechanical properties of the mild steel to copper bronze joint by friction welding method have never been reported up-to-date. Thus, the aim of this study is to examine the mechanical properties and optimal welding conditions of friction welded joints of ASTM B22 Tin bronze and AISI 1010.

Materials and Methods

Chemical composition of the copper-based bronze and mild steel employed is given in Table 2. Cylindrical test specimens of 20 mm in diameter and 100 mm in length were prepared for friction welding. Before friction welding, the surfaces facing each other were machined using a lathe. Before welding, the surface of the workpieces were cleaned with a stainless steel brush and acetone to remove the oxide layer and stains. Joining of these two dissimilar alloys was performed on a continuous drive friction welding machine of 250 kN capacity at a constant rotation speed of 2500 rev/min, and constant friction time of 3 s. Friction and upset pressures can be observed on the screen, and the welding sequence stages are controlled by a solenoid valve. The welding parameters were as follows: friction pressures (P_1): 10, 15, 20 MPa; upset pressures (P_2): 22, 25, 30 MPa; and upset (forging) time (t_1) of 1, 5, 7, 8 s. Tensile test specimens were prepared according to ASTM E8M-00b. Ultimate tensile strength (UTS) and yield strength of the welded specimens were determined. Hardness values ($VH_{0.5}$) were determined by using a Zwick 3212 device. Measurements were taken in the welding center through base metals. For tensile strength and hardness test values, at least three specimens were carried out for each parameter. The axial shortening was estimated by measuring the length of the specimens before and after welding. The microstructure was investigated by optical microscopy. The steel specimens were polished and etched with a solution consisting of 70% HCl and 30% HNO_3. The grains have equaxied shapes ranging from 30 to 150 µm in dimension. The bronze specimens were also polished and etched with a solution consisting of 40% NH_4OH, 60% H_2O. Typical microstructures of materials can be seen in Fig. 1A, B.

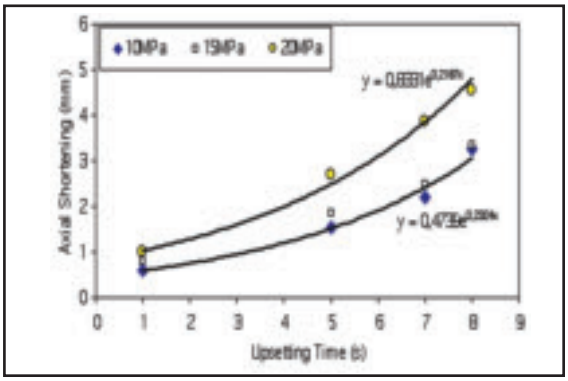

Fig. 2 — The effect of upset time and friction pressure on the axial shortening with 22 MPa upset pressure.

Results and Discussions

Effects of Welding Parameters on Axial Shortening

The effect of upset time and friction pressure on the axial shortening is presented in Fig. 2. Similarly, the effects of upset time and pressure on axial shortening are also shown in Fig. 3. It is clearly seen that axial shortening significantly increased with increasing friction, upset pressures, and times. To ensure good metallurgical integrity, it is necessary to break up and expel the contaminated surface layers. In rotary friction welding, this is achieved with greater pressure and upset times. Also, in light of these figures, the axial shortening exponentially increased by increasing these welding parameters. The fit of the results yields the following simple formula:

$$A_S = 0.4 - 0.8\, t^{0.22} \qquad (1)$$

where A_S is the axial shortening (mm) and

Table 1 — Some Physical and Mechanical Properties of Mild Steel and Copper Bronze

Properties	Unit	AISI 1010	ASTM B22
Density	g/cc	7.87	8.72
Themal Conductivity	W/m-K	51.9	74
CTE	µm/m-°C	12.2	20
Ultimate Tensile Strength	MPa	425	310
Yield Strength	MPa	180	150
Elongation	%	28	25
Elastic Modulus	GPa	200	105
Melting Temperature	°C	1535	1000
Hardness	Hv	100	83

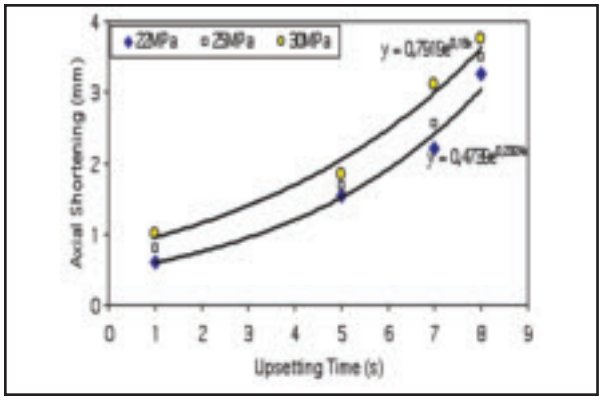

Fig. 3 — The effect of upset time and pressure on the axial shortening with 10 MPa friction pressure.

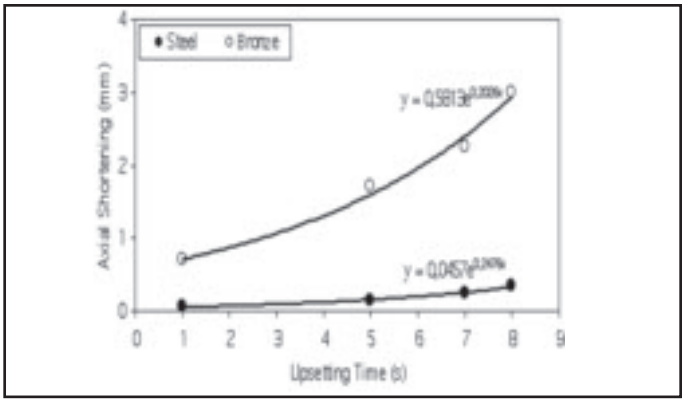

Fig. 4 — Typical axial shortening against upset time graph with 15 MPa friction pressure and 22 MPa upset pressure.

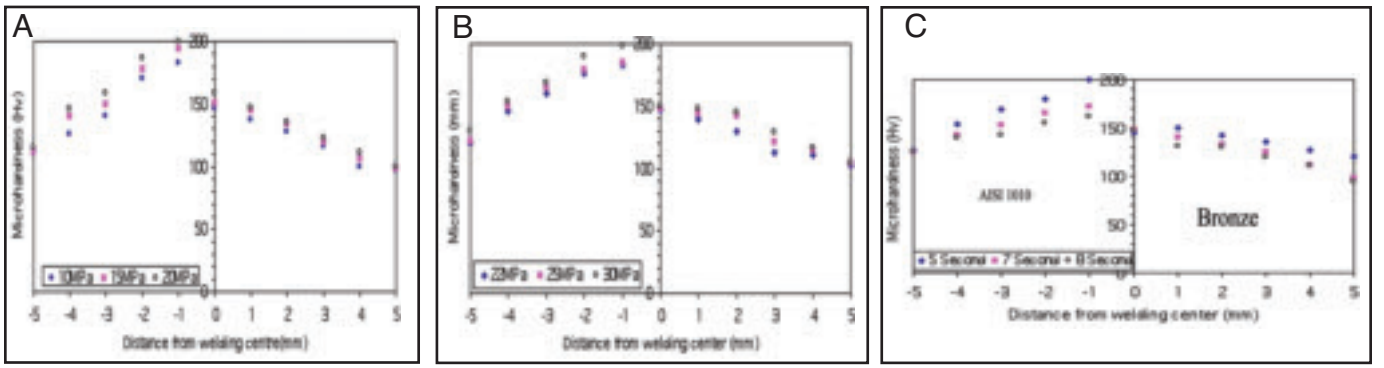

Fig. 5 — The microhardness distribution of materials. A — The effect of friction pressure (P_2 = 22 MPa, t_1 = 5 s); B — the effect of upset pressure (P_1 = 10 MPa, t_1 = 5); C — the effect of upset time (P_1 = 10 MPa, P_2 = 30 MPa).

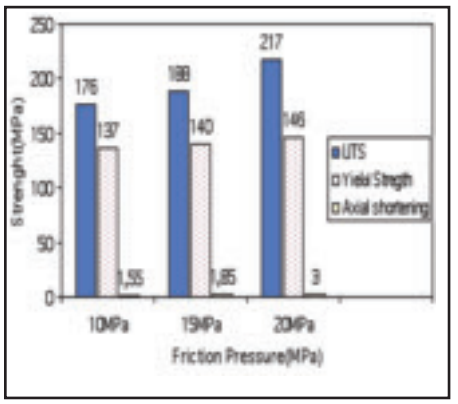

Fig. 6 — The effect of friction pressure on the tensile response of the 22 MPa upset pressure at 5 s upset time.

t is the upset time (s). This formula can clearly explain the change of axial shortening with the upset time under the welding conditions in this study. However, this basic equation is primitive, and further experimental study should be done to incorporate the factors related to material physical and some mechanical properties. At the low friction and upset pressures, the friction heat is not enough to soften the interfacial materials; and the interface temperature is relatively low due to low heat input. As time increases, the friction and contact area also significantly increases the heat generation on the interfaces, and in return flash is formed. Hence, axial shortening increases remarkably with the interface temperature rise and softening of materials following the extruding process under the rotary motion. Therefore, upset friction pressures and times are key parameters in controlling the formation of a perfect joint. Sathiya et al. (Ref. 11) found that in the case of stainless steel, a combination of high friction, upset pressure, friction time, and upset time produced more axial shortening (melt-off) that played an important role in the mechanical properties. They observed that increased axial shortening resulted in better mechanical properties of joints. In general, the mechanical properties of a weld are more closely related to the axial shortening rate, which can also be a factor indicative of joint quality.

Figure 4 shows the effect of the materials on axial shortening. The different thermal and physical properties of the materials to be welded in dissimilar metal welding (heat capacity, thermal conductivity, relationship between hardness and temperature) generally result in asymmetrical deformation. In this study, during the friction welding of steel to bronze, a flash forms mostly on the bronze side. While the axial shortening increased exponentially for the bronze materials, the steel showed a linear increase in axial shortening. Although both materials were axially shortened with increasing upset times, shortening of the bronze material was more pronounced compared with steel. It is well known that bronze melting temperature and yield strength are significantly low, and thermal conductivity and coefficient of thermal expansion are quite high, compared to steel. Thus, more bronze materials will be softened during the welding process due to the extensive plastic deformation, and relatively high temperature occurs on the joint surface. Hence, more bronze materials deformed plastically due to the decreased yield strength (effect of the high temperature) compared to the steel. The heat generation in the joint surface is significantly different from center to outer shell. This fact suggests that the extrusion rates of ma-

Table 2 — Chemical Compositions of Copper Bronze and Mild Steel

Material	Sn	Zn	Pb	Ni	Fe	Cu
ASTM B22	10	1.14	0.5	0.16	0.04	remain
		Elements wt-%				
Material	C	Mn	Ni	Cr	Si	Fe
AISI 1010	0.1	0.3	0.22	0.1	0.04	remain

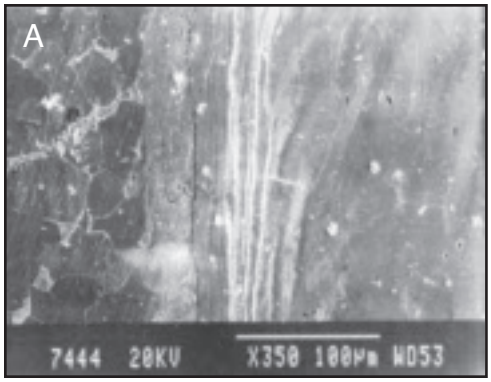

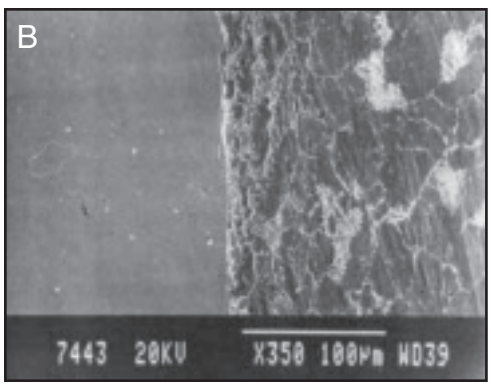

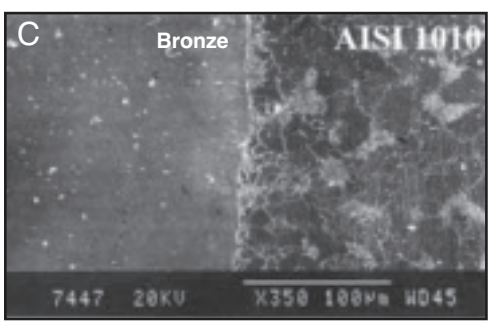

Fig. 7 — The effect of friction pressure on the microstructure. A — P_1 = 10 MPa, P_2 = 22 MPa, t_1 = 5 s. B — P_1 = 15 MPa, P_2 = 22 MPa, t_1 = 5 s. C — P_1 = 20 MPa, P_2 = 22 MPa, t_1 = 5 s.

terials in the middle and edges will have different microstructures in both specimens owing to the nonuniform temperature distribution. In friction welding, the temperature would be minimum at the center and maximum at the periphery because more intermixing takes place at the peripheral region of the weld. Thus, the maximum heat generation point occurred somewhere close to the periphery beneath the surface of dissimilar metals (Ref. 12). In addition, the flash was found to increase not only with the increase in friction welding parameters but also with the density of bronze. Similar results were also reported by Jayabharath et al. (Ref. 13). Furthermore, for a dissimilar weld in rheology and geometry, computer simulation demonstrates that the weaker material is thicker than the stronger part, which leads to different flash shapes and relative upset (Ref. 14).

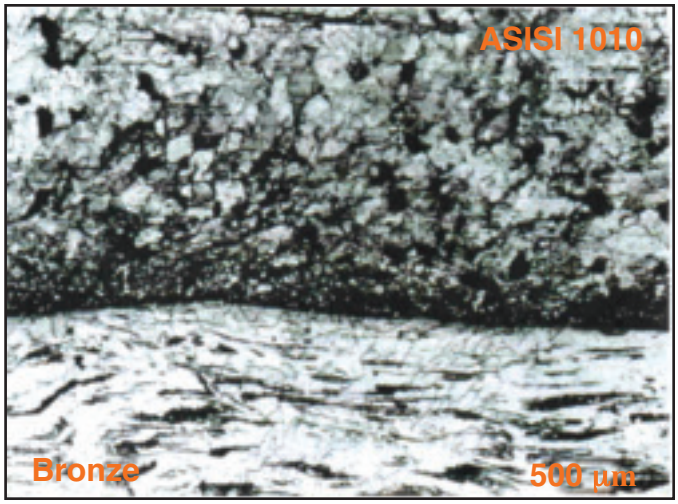

Fig. 8 — Microstructural changes inside the welding region.

Hardness Distribution

Figure 5A shows the effect of friction pressures, B shows the effect of upset pressures, and C shows the effect of upset time on the hardness distribution in the direction perpendicular to the weld interface of the as-welded specimen. As can be seen from these figures, almost the same trend was observed in the microhardness profiles of all samples. The maximum hardness values of joints were obtained on the steel side next to the welding centerline. The hardness values generally increased with increasing friction pressure and upset pressures, but hardness values decreased with increasing upset time. Increasing hardness in the welding interface can be related to the microstructure formed in the weld interface as a result of the heat input and plastic deformation. As can be seen from Table 1, the hardness of bronze is 83–96 Hv, but, the weld interface hardness is measured around 147 Hv. Similarly, the hardness value of mild steel is 100–118 Hv, but the welding interface is measured around 200 Hv. It can be said that microstructural evaluations around the interface, diffusion of elements on the sides, work hardening, dislocation density, grain refinement, and formation of precipitations may have caused this increase. Although work hardening is also effective on the hardening in the bronze side, hardening in steel is mostly a direct result of fine grains, rapid cooling from the welding temperature, and formation of precipitates. A similar hardness profile was also observed for dissimilar material couples (Refs. 11, 15, 16). It can be said that the hardness properties are influenced by an interactive effect of friction, upset pressures, and upset times, which are combinations of heat input and a degree of strain hardening.

Tensile Strength

The influence of friction pressure on the tensile test result is shown in Fig. 6. From the data, it may be noted that UTS and yield strength increased with an increase in friction pressure and axial shortening. The UTS strength corresponds to about 70% that of the bronze part and 50% that of the steel. Nearly full performance can be obtained for the yield strength of the bronze material that was tested on the highest friction pressure and the highest axial shortening. In general, tensile strength increased up to a certain value with increasing friction pressure and then decreased slightly after reaching the optimum value. This reduction is probably due to flashing of the heated soft material from the interface on upset pressure. Flashing increases with increasing friction pressure (Ref. 17). Joints performed here were quite brittle in nature and either in the HAZ region of the bronze or joint interface. This can be attributed to the diffusivity of Fe that is higher than that of Cu and hence a reaction layer can be formed toward the bronze side and the failure has taken place in this zone.

Microstructure

Figure 7A–C shows the microstructural features of interfaces with increasing friction pressure. It is clearly seen that insufficient friction pressure on the joining surface resulted in an inadequate locking of the surfaces (Fig. 7A) where limited plastic deformation and microstructural changes occurred, and these facts caused poor tensile response of the joint. An increase in the friction pressure caused better joining surfaces (Fig. 7B, C) where recrystallization occurs on the bronze side, and grain refinement and strain hardening occurs on the steel side. The width of the recrystallized region is mainly affected by the friction pressure. An increase in the

friction pressure resulted in a wider fine grain region. A change in microstructure and axial shortening also notably occurred in the bronze side. The same phenomenon has been reported during friction welding of dissimilar welds, namely Fe-Ti, Cu-Ti, Fe-Cu, Fe-Ni (Ref. 12). The recrystallized region of Fig. 7C decreases compared to that of Fig. 7A, and fracture occurred in the faying surface. However, tensile fracture of the joint (Fig. 7C) did not occur in the faying surface but in the bronze side of the HAZ. This means that the decrease in recrystallized region was caused by high friction pressure that contributes to better tensile strength. Heat flow occurs preferentially in the material with the greatest thermal conductivity. Due to the different thermal conductivities between bronze and steel, the specific heat is so large, and hence, most of the frictional heat was generated in bronze. The difference in thermal conductivity explains the microstructural changes that occur preferentially in the bronze side. Similar microstructural observations for the Cu-Ti couples were also reported in Ref. 18. Most of the changes occurred preferentially in the copper, no evidence of microstructural variation was seen in the vicinity of the interface, neither grain growth nor grain boundary precipitation was observed. They attributed this behavior to the difference in thermal conductivity (Ref. 18). It can be said that for the perfect interfacial bonding, sufficient upset time and friction pressures are necessary to reach the optimal temperature and severe plastic deformation to bring these materials within the attraction range. Sathiya et al. (Ref. 11) found that in the case of stainless steel, a combination of high friction, upset pressure, and high upset time produced high tensile strength and high impact values. A bond quality classification system was developed using a novel, noncontact, acoustic emission sensing technique. An efficient, inexpensive, and fast production benefit can be achieved by using process monitoring systems (Refs. 19, 20).

Figure 8 shows the microstructural changes of the bronze and steel sides of the weld. During the friction weld process, the temperature near the weld interface would reach just below A_1 temperature, which is about the recrystallization temperature for the mild steel. Therefore, very fine equaxied grains formed from ferrite and pearlite. A martensitic structure can even be seen in this region when the weld interface reaches above the A_3 temperature with the occurrence of rapid cooling (Ref. 21). Beyond this region, elongated and severely compressed grains can be seen in the HAZ region of the steel. However, for the bronze side, there was no fine grain next to the interface, but partially melted zones and fibrous elongated grains were evident along the rolling direction. The intensity of orientation was found to be dependent on the welding parameters (Ref. 17).

Conclusions

To clarify the feasibility of friction welding to AISI 1010-ASTM B22 copper bronze, the characteristic of structures, tensile properties, hardness values, and microstructural changes of friction joints were investigated with various welding parameters. The main conclusions are summarized as follows:

1. Friction welding can be used successfully to join mild steel to bronze. The processed joints exhibited better mechanical and metallurgical characteristics as compared to those made with fusion welding techniques.

2. The tensile strength of the obtained weld joints can reach a base metal strength of 70% if suitable welding parameters are determined. Fracture usually occurs either in the HAZ of soft material or in the joint surface.

3. The axial shortening exponentially increased by increasing the upset time. The best fit of data yields a formula: $A_S = 0.4 - 0.8\, t^{0.22}$.

4. Upset time, friction time, and axial shortening play important roles in the metallographic structure and mechanical response of the weld.

5. Extensive deformation is confined mostly to the bronze side due to their low flow stress and high thermal conductivity.

6. Higher hardness values are observed next to the interface, but they dramatically decreased with increasing distance and upset time.

7. An increase in the friction and upset pressure result in slightly higher hardness values.

8. Typical microstructural features were observed in the welding region. Recrystallized fine and elongated grains were evident adjacent to the joint surface.

9. For this study, the optimal joint performance was attained at a friction pressure of 20 MPa, upset pressure of 22 MPa, and upset time of 5 s.

Acknowledgments

The authors wish to thank Prof. Dr. G. Said and H. Ozden for their valuable contributions. Also, special thanks to Turkish Track Factory for its support and guidance during the experimental stage.

References

1. Uygur, I., and Gulenc, B. 2004. The effect of shielding gas composition for MIG welding process on mechanical behaviour of low carbon steel. *Metalurgija* 43(1): 35–40.

2. Uygur, I. 2006. Microstructure and wear properties of AISI 1038H steel weldments. *Industrial Lubrication and Tribology* 58(6): 303–311.

3. Uygur, I., and Dogan, I. 2005. The effect of TIG welding on microstructure and mechanical properties of a butt-joined unalloyed titanium. *Metalurgija* 44(2): 119–123.

4. *www.matweb.com*

5. Uygur, I. 2007. Microstructure and performance in diffusion welded joints of Al 5-10-15% WCp composites. *Materials Science Forum* 546–549: 671–674.

6. Kurt, A., Uygur, I., and Ates, H. 2007. Effects of temperature on the weldability of powder metal parts joined by diffusion welding. *Materials Science Forum* 546–549: 667–670.

7. Kurt, A., Uygur, I., and Mutlu, E. 2006. The effect of allotropic transformation temperature in diffusion-welded low carbon steel and copper. *Metallofiz., Noveishie Tekhnol.* 28(1): 39–52.

8. Kurt, A., Uygur, I., and Ates, H. 2007. Effect of porosity content on the weldability of powder metal parts produced by friction stir welding. *Materials Science Forum* 534–536: 789–792.

9. Vairis, A., and Frost, M. 1999. On the extrusion stage of linear friction welding of Ti_6Al_4V. *Mater. Sci. Eng. A* 271: 477–484.

10. Li, W. Y., Ma, T. J., Yang, S. Q., Xu, Q. Z., Zhang, Y., Li, J. L., and Liao, H. L. 2008. Effect of friction time on flash shape and axial shortening of linear friction welded 45 steel. *Materials Letters* 62: 293–296.

11. Sathiya, P., Aravidan, S., and Noorul Haq, A. 2007. Effect of friction welding parameters on mechanical and metallurgical properties of ferritic stainless steel. *Int. J. Adv. Technol.* 31: 1076–1082.

12. Meshram, S. D., Mohandas, T., and Reddy, G. M. 2007. Friction welding of dissimilar pure metals. *J. Mater. Proces. Techn.* 184: 330–337.

13. Jayabharath, K., Ashfaq, M., Veugopal, P., and Achar, D. R. G. 2007. Investigations on the continuous drive friction welding of sintered powder metallurgical (P/M) steel and wrought copper parts. *Materials Sci. & Eng. A* 454: 114–123.

14. D`Alvise, L., Massoni, E., and Walloe, S. J. 2002. Finite element modelling of the inertia friction welding process. *J. Mater. Process. Techn.* 125–126: 387–391.

15. Ozdemir, N., Sarsilmaz, F., and Hascalik, A. 2007. Effect of rotational speed on the interface properties of friction-welded AISI 304L to 4340 steel. *Mater. & Design* 28: 301–307.

16. Sahin, M. 2009. Joining of stainless-steel and aluminum materials by friction welding. *Int. J. Adv. Manuf. Techn.* 41(5–6): 487–497.

17. Ates, H., Turker, M., and Kurt, A. 2007. Effect of friction pressure on the properties of friction welded MA956 iron-based superalloy. *Mater. & Design* 28: 948–953.

18. Kim, S. Y., Jung, S. B., and Shur, C. C. 2003. Mechanical properties of copper to titanium joined by friction welding. *J. Mater. Scien.* 38: 1281–1287.

19. *www.boulder.nist.gov/div853/Events%20%20Welding%20Conference/Weld_Papers/1-1%20Hartman-paper.pdf*

20. *library.lanl.gov/cgi-bin/getfile?00818853.pdf*

21. Sahin, M., Akata, H. E., and Ozel, K. 2008. An experimental study on joining of severe plastic deformed aluminum materials with friction welding method. *Mater. & Design* 29(1): 265–274.